Electronic Supplementary Material (ESI) for Nanoscale.
This journal is © The Royal Society of Chemistry 2017

Supporting Information for

High performance bi-layer atomic switching device

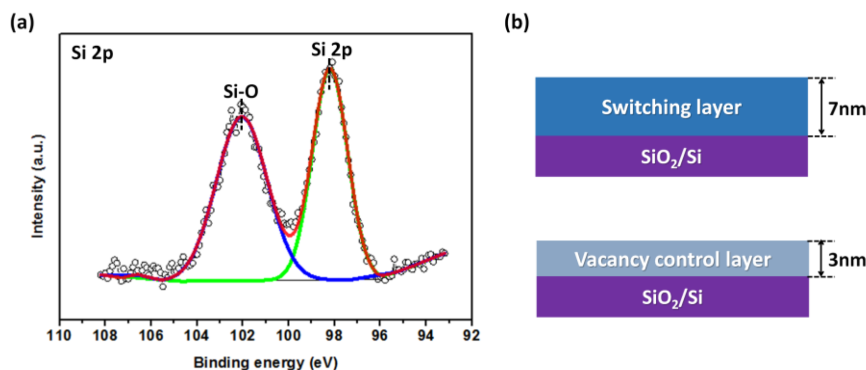

Figure S1. (a) Si 2p XPS result for the VCL. (b) Schematic diagrams of the switching layer (SL) and the vacancy control layer (VCL) in the XPS samples.

The O 1s peak due to Si-O bonding was only detected in the XPS sample for the supply layer. This result arises because the supply layer is thinner than the switching layer, and the peaks of the substrate are detected together. It is re-confirmed by the Si 2p peaks for the VCL in Figure S1a. A clear Si-O peak (102 eV) and a clear Si peak (98 eV) are evident, whereas no such peaks arise for the SL.

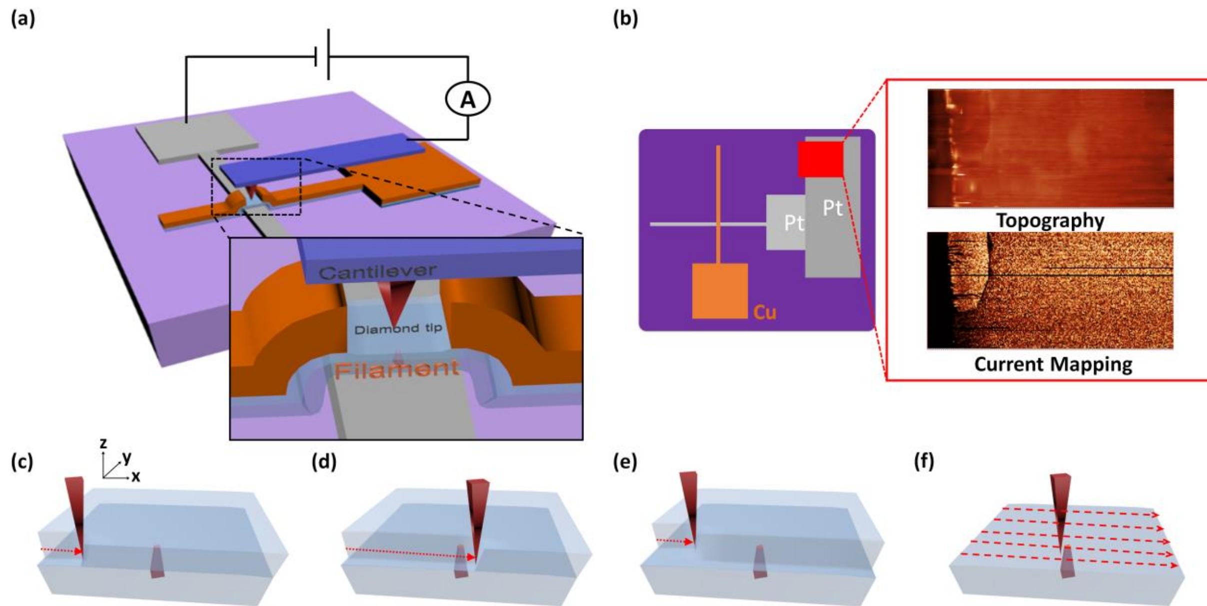

Figure S2. (a) A schematic diagram of the C-AFM measurement set-up. (b) Top view of the set-up, showing an experimental topographical image and a current map of the extended bottom electrode. (c)-(e) Each step of the nanolithography etching process. (f) C-AFM measurement after the etching process

In order to verify the results, we obtained with C-AFM, we first measured the current in the extended bottom electrode of a device that had already been turned on. The successful operation of our C-AFM set-up was then confirmed by matching the electrode shape in the topography image with the shape of the map of the current at a reasonable current level (~nA).

Figure S2 c-e show each step of the etching process. The diamond tip presses the sample surface with optimized set point value and scans a line along with the x-axis direction. After finishing this line scanning, the tip is lifted up to its original height, moving in the y-direction from the starting point, pushed down again with the set point value and scratches in the x-direction. By repeating this process, the designated area of the surface was etched. C-AFM was performed after etching 3 nm from the top of the SL with a set point value of about 550 nN. (Fig. S3 f)

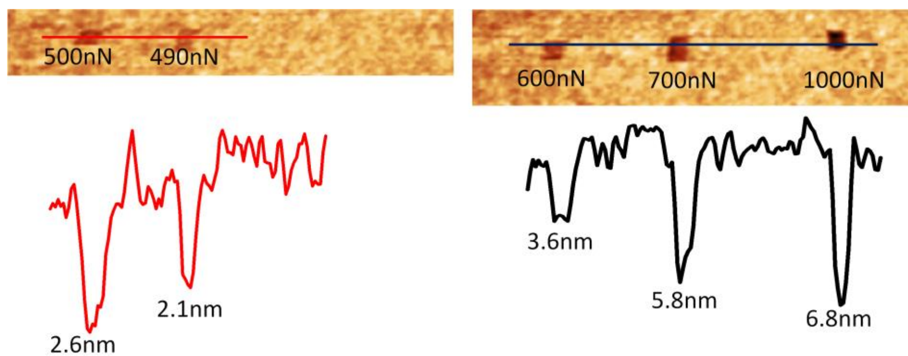

Figure S3. Topographical images of the tantalum oxide film after nanolithography.

Figure S3 shows depth profiles after nanolithography with various set point forces. A diamond-coated tip was used because of the need to scratch the hard oxide materials. We also chose a probe with a large spring constant (42 N/m). If this constant is low, the cantilever of the probe will be flexible and be unable to apply enough force to scratch the material. To scratch the surfaces of the samples, the feedback of the z-axis scanner was turned off. As the applied force increases, the scratch depth of the film also becomes deeper.

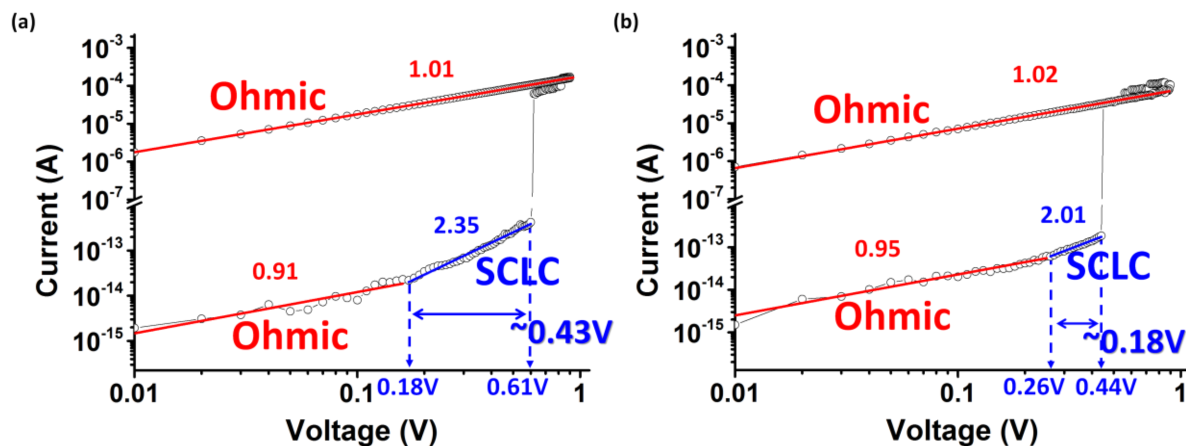

Figure S4. I-V curves for the single-layer device (a) and the bi-layer device (b) during the set processes.

Figure S4 a and b are plotted on the double logarithmic scale. These curves were fitted with equations related to the two types of current conduction mechanisms. The current due to ohmic conduction is proportional to the voltage ($J = ne\mu\frac{V}{d}$, $I \propto V$). Thus, the slope of the line in the I-V curve of the double logarithmic scale is 1. However, as the voltage increases, the slope becomes approximately 2. A higher applied bias means that the induced charges accumulate on the electrodes and that the electric field due to these charges affects current conduction. This effect is known as space-charge-limited conduction (SCLC, $J = \frac{9}{8}\varepsilon\mu\frac{V^2}{d^3}$, $I \propto V^2$). The red and blue lines in each graph are the lines fitted with the ohmic conduction and SCLC equations respectively. It is evident that the SCLC line of the bi-layer device is shorter than that of the single-layer device, which means that the conduction due to space charges is more suppressed in the bi-layer device. This suppression probably arises because the charges generated to compensate for the oxygen vacancies supplied from the supply layer screen the effects of the excess injected carriers.[1]

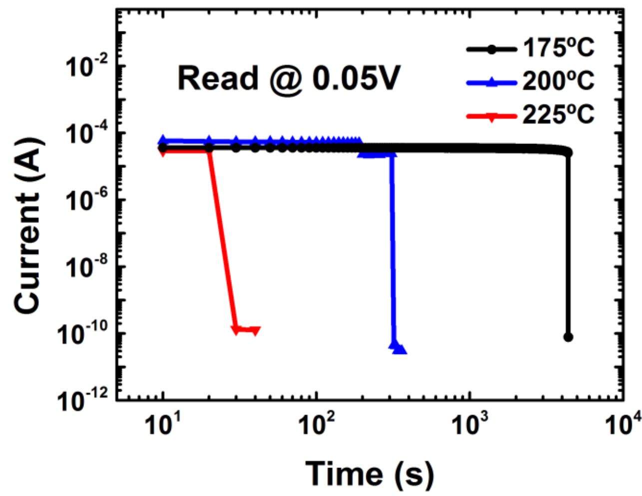

Figure S5. Typical failure time curves measured at various temperatures to obtain the results for the MTTF curve.

Reference

1. S. Bhattacharyya, A. Laha and S. B. Krupanidhi, *Journal of Applied Physics*, 2002, **91**, 4543-4548.